ELSEVIER

Journal of Alloys and Compounds 320 (2001) 108–113

Journal of ALLOYS AND COMPOUNDS

www.elsevier.com/locate/jallcom

Effect of aluminum substitution and rare-earth content on the structure of $R_2(Fe_{1-x}Al_x)_{17}$ (R=Tb, Dy, Ho, Er) phases

T. Yanson[a], M. Manyako[a], O. Bodak[a], R. Cerny[b], K. Yvon[b,*]

[a]*Ivan Franko National University of L'viv, L'viv, Ukraine*

[b]*Laboratoire de Cristallographie, Université de Genève, 24 quai Ernest Ansermet, CH-1211 Genève, Switzerland*

Received 11 January 2001; accepted 19 January 2001

Abstract

The phase equilibria in the iron rich parts of the R–Fe–Al (R=Tb, Dy, Ho, Er) phase diagrams at 500°C have been studied by X-ray powder diffraction analysis. As the aluminum contents in the series $R_2(Fe_{1-x}Al_x)_{17}$ are increased the hexagonal Th_2Ni_{17} type structure (or a substitution derivative of that structure) transforms — usually via a hexagonal $TbCu_7$ type derivative structure — into the rhombohedral Th_2Zn_{17} type structure (or a substitution derivative of that structure). The hexagonal structures dominate at or below the molar ratio R/(Fe,Al)=2/17 (10.5 and 9.5 at.% R), while the rhombohedral structure dominates at higher R contents (11.5 at.%). The solubility of aluminum in the hexagonal structure increases as the atomic size of R decreases (from x=0–3.42 in $Tb_2Fe_{17-x}Al_x$ to x=0–4.75 in $Er_2Fe_{17-x}Al_x$), while that in the rhombohedral structure decreases (from x=7.70–9.41 in $Tb_2Fe_{17-x}Al_x$ to x=5.70–7.03 in $Er_2Fe_{17-x}Al_x$). The cell parameters suggest that the nature of the atomic substitutions in the various crystal structures changes as a function of both structure type and atomic size of R.

Keywords: Phase diagrams; Rare-earth iron aluminides; Ferromagnetic compounds

1. Introduction

The so-called R_2Fe_{17} (R=rare earth) compounds and their substitutional derivatives, in particular those in which iron is partially replaced by aluminum, are of interest because of their ferromagnetic properties (Ref. [1] and references therein). The binary compounds occur with two major crystallographic modifications, the rhombohedral Th_2Zn_{17} type structure for light R elements (Ce–Sm) and the hexagonal Th_2Ni_{17} type structure for heavy R elements (Dy–Lu) and Y. Some R elements (Tb, Gd) give rise to both modifications [2]. The switchover from the hexagonal to the rhombohedral structure is generally attributed to geometrical factors. This is in line with the observation [3] that substituting Fe by ternary elements of bigger atomic size such as Al stabilizes the rhombohedral structure. Work on the aluminum substituted series $R_2Fe_{17-x}Al_x$ (R=Tb, Dy, Ho, Er) has shown that the hexagonal structure exists for Al contents of up to x=1 (Tb [4]), 3.91 (Dy [5]), 3 (Ho [6], Er [1]) and the rhombohedral structure for Al contents in the ranges x=1.98–8.12 (Tb [4]), x=4.93–6.97 (Dy [5]), x=4–10 (Ho [6]), x=4–9 (Er [1]). The solubility of aluminum generally increases as the annealing temperature is decreased. Little is known, however, about the phase relations outside the molar ratio R/(Fe,Al)=2/17 [3]. The aim of the present work was to investigate these relations for R=Tb, Dy, Ho, Er at R compositions below and above the 2/17 ratio, and at a low annealing temperature (500°C). This knowledge is of importance for the assignment of ferromagnetic properties and their optimization. It will be shown that the solubility of Al in the hexagonal and rhombohedral phases depends not only on temperature but also on R content. It will also be shown that a new phase appears at Al concentrations intermediate to those of the hexagonal and the rhombohedral phases that has a hexagonal $TbCu_7$ type derivative structure.

2. Experimental

For each of the R–Fe–Al systems studied (R=Tb, Dy, Ho, Er) three series of samples of general compositions $R_2(Fe_{1-x}Al_x)_{17}$ were synthesized, one at an R content of 10.5 at.%, i.e. at the nominal composition $R_2Fe_{17-x}Al_x$,

*Corresponding author. Tel.: +41-22-702-6231; fax: +41-22-781-2192.

E-mail address: klaus.yvon@cryst.unige.ch (K. Yvon).

0925-8388/01/$ – see front matter
PII: S0925-8388(01)00930-6

and two at lower and higher R contents of 9.5 and 11.5 at.%, respectively. The aluminum contents were increased in intervals of 2.5 at.% up to 50 at.%. In order to establish phase equilibria some samples were also prepared at 5 and 15 at.% R. A total of 260 samples weighing ~1 g each were prepared by arc-melting ingots and/or pieces of compacted powders of the constituting elements of at least 99.9% purity in a water cooled copper crucible under purified argon atmosphere. The reaction products were remolded several times to ensure homogeneity, and annealed in evacuated quartz tubes at 500°C for 720 h. After quenching in cold water they were investigated by X-ray powder diffraction (Fe Kα radiation). At least three major phases could be identified, one having the hexagonal Th_2Ni_{17} type structure (or a substitution derivative of that type, called 2/17H hereafter), a second having the rhombohedral Th_2Zn_{17} type structure (or a substitution derivative, called 2/17R hereafter), and a third having the hexagonal $TbCu_7$ type structure (or a substitution derivative, called 1/7H hereafter). The occurrence of these three phases in the sections investigated (9.5, 10.5 and 11.5 at.% R) is represented in the partial phase diagrams shown in Fig. 1, and the crystallographic parameters of their corresponding subcells are shown in Fig. 2. Various difficulties occurred while establishing these phase diagrams. Firstly, since the three structures are closely related and have common subcells (2/17H: $a/\sqrt{3}$, $c/2$; 2/17R: $a/\sqrt{3}$, $c/3$; 1/7H: a, c) their X-ray patterns showed extensive line overlap. Secondly, the structural differences induced by the various substitutions are not very pronounced. Thus the

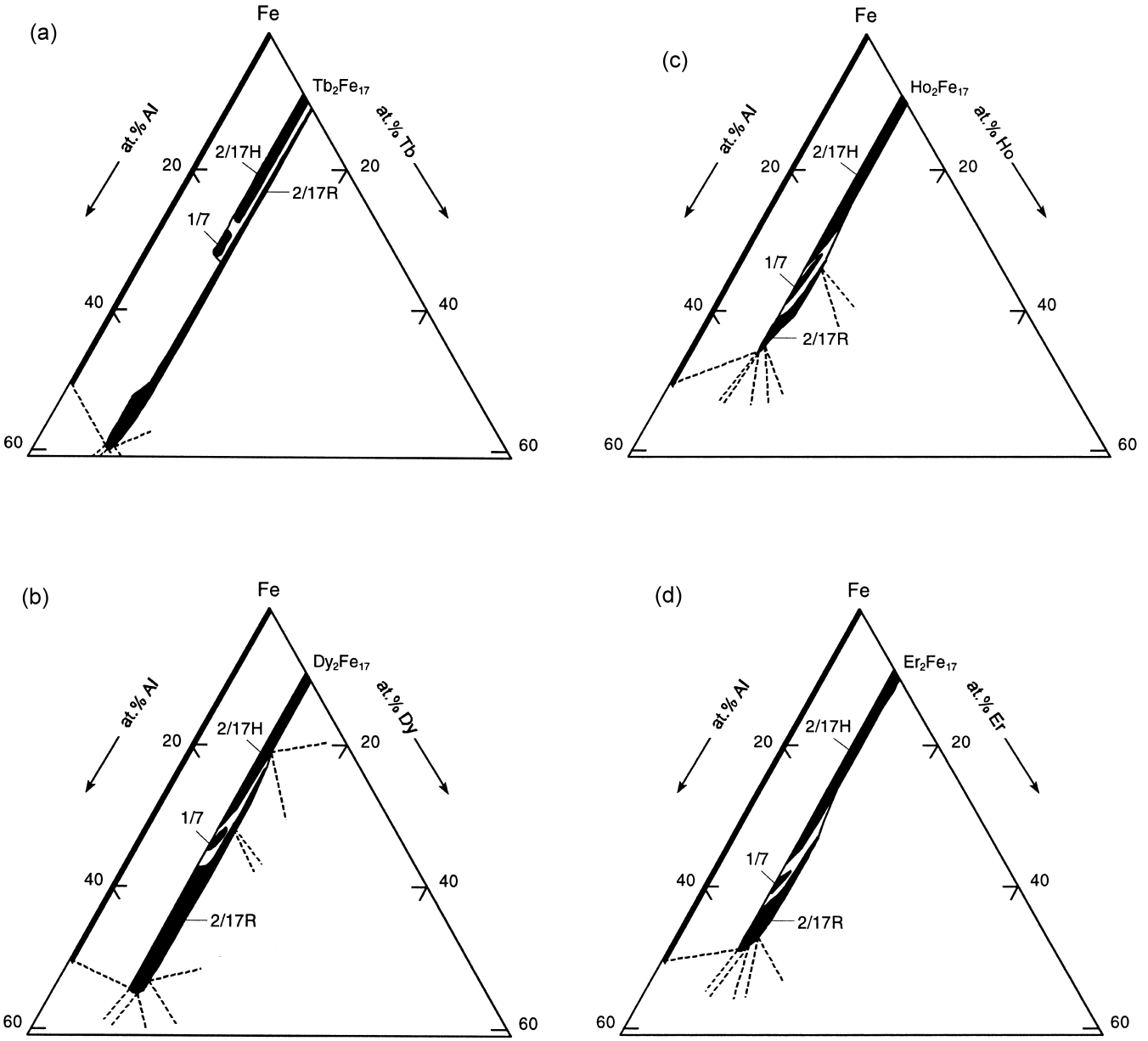

Fig. 1. Isothermal section at 500°C of the iron rich part of the systems Tb–Fe–Al (a), Dy–Fe–Al (b), Ho–Fe–Al (c) and Er–Fe–Al (d).

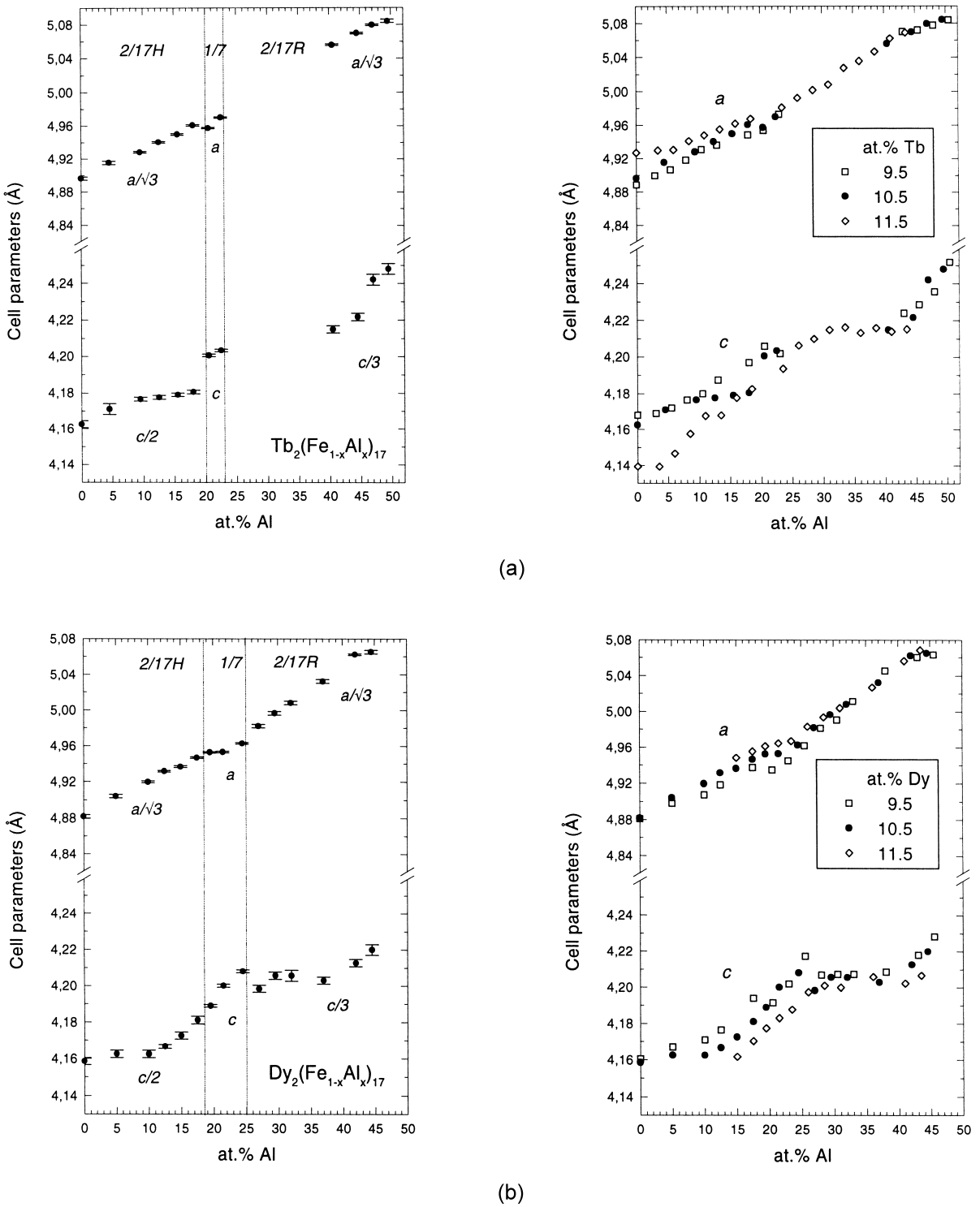

Fig. 2. Crystallographic subcell parameters *a* and *c* as a function of Al content for the 2/17H, 1/7H and 2/17R phases in the MR phase field for Tb (a), Dy (b), Ho (c) and Er (d) at 10.5 at.% R (left) and other R concentrations (right).

phase identification relied on relatively small details in the diffraction patterns and did not allow one to identify the presence of other closely related structure variants, such as for example the rhombohedral $PrFe_7$ type or the hexagonal $LuFe_{9.5}$ type structures. Furthermore, due to extensive structural disorder the exact compositions of the various phases could not be derived in an independent manner from crystal structure refinements. Those referring to single-phase regions were assumed to correspond to the nominal composition of the sample. Finally, in spite of the

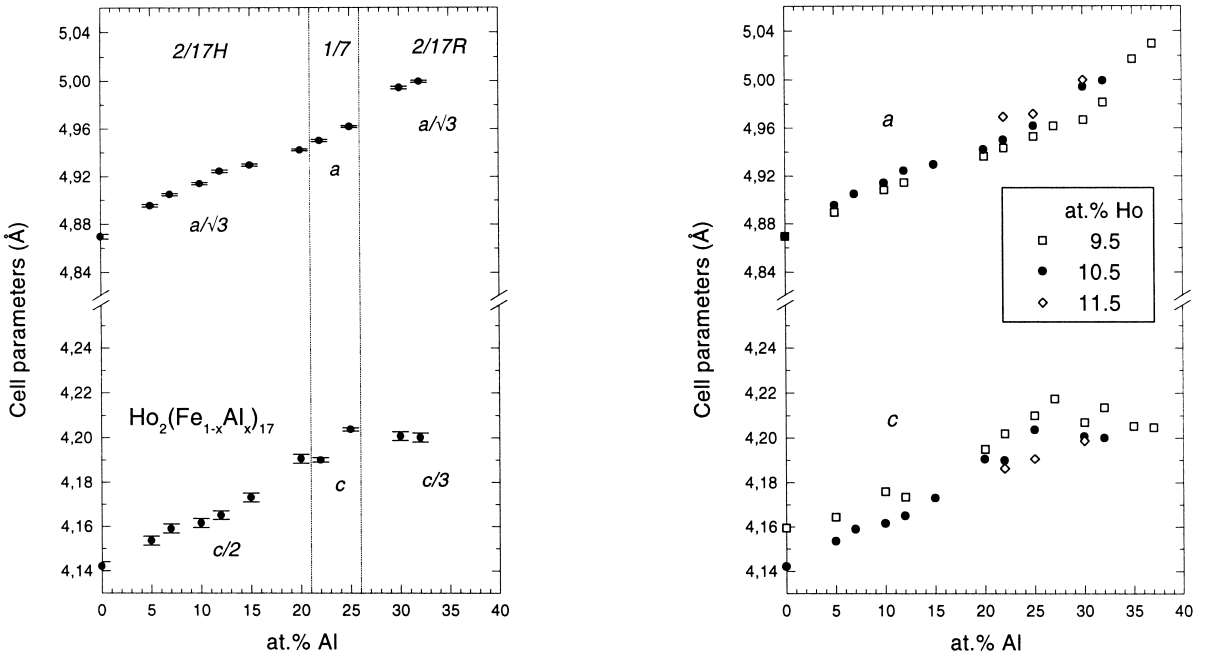

(c)

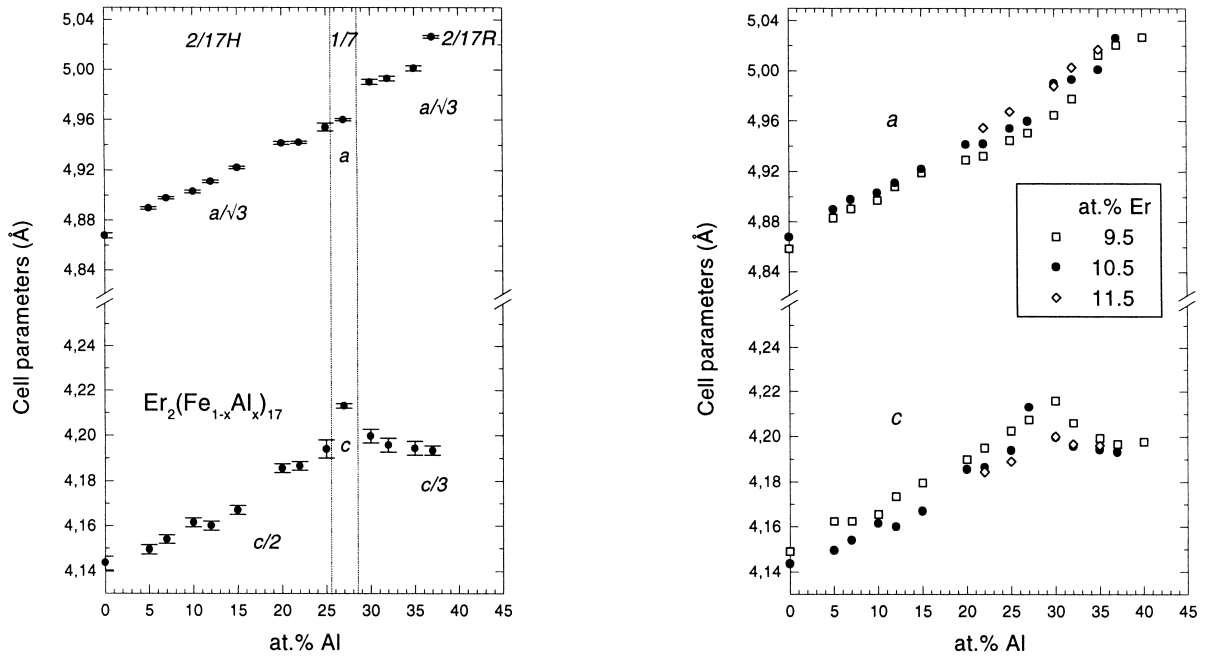

(d)

Fig. 2. (*continued*)

relatively fine compositional grid chosen, experimental evidence for two phase regions between the various ternary phases could generally not be obtained. Thus, for the purpose of simplicity the overall region in the phase diagrams in which these ternary phases occurred was designated ‘mixed region’ (MR), similar to Ref. [7].

3. Results and discussion

The iron rich corners of the R–Fe–Al (R = Tb, Dy, Ho, Er) phase diagrams contain at least three phases of approximate composition $R_2Fe_{17-x}Al_x$, one (2/17H) at low, another (1/7H) at intermediate, and a third (2/17R)

at high aluminum concentrations. The systematic appearance of the 'intermediate' 1/7H phase in these systems has so far not been reported. All phases are clearly not limited to the molar ratio R/(Fe,Al)=17 but extend to both lower and higher R contents. The compositional limits of the MR phase field, the detailed phase equilibria and the cell parameter ranges differ from one system to another.

3.1. Tb–Fe–Al system

At a terbium content of 9.5 at.% (Tb/(Fe,Al)<2/17) the 2/17H, 1/7H and 2/17R phases cover the concentration ranges 0–18, 20.5–23 and 43–50.5 at.% Al, respectively (Figs. 1a and 2a). At a Tb content of 10.5 at.% (Tb/(Fe,Al)=2/17) they cover the concentration ranges 0–18, 20.5–22.5 and 40–49.5 at.% Al, respectively, i.e. their maximum Al contents decrease. At a Tb content of 11.5 at.% (Tb/(Fe,Al)>2/17) only the 2/17R phase exists and it covers the concentration range 0–43.5 at.% Al. The phases of the MR phase field are in equilibrium with the solid solutions Fe(Al) $Tb(Al,Fe)_2$ and $Tb(Fe,Al)_{12}$ and a non-identified ternary phase (not shown). As to the binary (aluminum free) phase it crystallizes with the 2/17H type structure at, or close to, the nominal composition Tb/Fe=2/17, and with the 2/17R type structure at higher Tb contents. As shown in Fig. 2a the cell parameters of the subcells generally increase with Al content and decrease with Tb content. Their rates of change do not differ much between the various structure types except for the *c* parameter of the 2/17R phase that increases more strongly than the *a* parameter.

3.2. Dy–Fe–Al system

At low and medium Dy contents (9.5 and 10.5 at.% Dy) the 2/17H phase covers the concentration ranges 0–23 and 0–19.5 at.% Al, respectively (Figs. 1b and 2b). Beyond these Al concentrations the 2/17H phase transforms first into the 1/7H phase (covering the ranges 25.5 at.% Al and 21.5–24.5 at.% Al, respectively), and then into the 2/17R phase (covering the ranges 28–45.5 at.% Al and 27–44.5 at.% Al, respectively). At high Dy contents (11.5 at.% Dy) only the 2/17R phase exists and it covers the concentration range 15–43.5 at.% Al. The MR phase field is in equilibrium with the solid solutions Fe(Al), $Dy(Al,Fe)_2$ and $Dy(Fe,Al)_{12}$, the binary compound Dy_6Fe_{23} (not shown), and ternary compounds having $MgZn_2$ and $ThMn_{12}$ type structures. As shown in Fig. 2b the parameters of the subcells generally increase with Al content and decrease with Dy content, and change more-or-less continuously between the various structures. However, in contrast to the Tb analogue the rate of increase of the *c* parameter of the 2/17R phase is smaller than that of the *a* parameter.

3.3. Ho–Fe–Al system

At low and medium Ho contents (9.5 and 10.5 at.% Ho) the 2/17H phase covers the ranges 0–27 and 0–20 at.% Al, respectively (Figs. 1c and 2c). Beyond these Al concentrations the 2/17H phase transforms first into the 1/7H phase (covering the ranges 30 at.% Al and 22–25 at.% Al, respectively) and then into the 2/17R phase (covering the ranges 32–37 at.% Al and 30–32 at.% Al, respectively). At high Ho contents (11.5 at.% Ho) only the 2/17R phase exists and it covers the range 22–30 at.% Al. The MR phase field is in equilibrium with the solid solutions Fe(Al), $Ho(Al,Fe)_2$ and $Ho(Fe,Al)_{12}$, and the ternary compounds having $ThMn_{12}$ and $MgZn_2$ type structures. As shown in Fig. 2c the parameters of the subcells generally increase with Al content and decrease with Ho content, except for the *c* parameter of the 2/17R phase that remains practically constant as the Al content is increased.

3.4. Er–Fe–Al system

At low and medium Er contents (9.5 and 10.5 at.% Er) the 2/17H phase covers the ranges 0–27 and 0–25 at.% Al, respectively (Figs. 1d and 2d). At higher Al contents it transforms into the 1/7H phase that covers the ranges 30–32 at.% Al and 27 at.% Al, respectively. At still higher Al contents the latter transforms into the 2/17R phase that covers the ranges 35–40 at.% Al and 30–37 at.% Al, respectively. At high Er contents (11.5 at.% Er) the 2/17R phase covers the range 22–35 at.% Al. The MR phase field is in equilibrium with the solid solutions Fe(Al), $Er_6(Fe,Al)_{23}$ and $Er(Al,Fe)_2$ and a ternary compound with $ThMn_{12}$ type structure. As shown in Fig. 2d the parameters of the subcell generally increase with Al content and decrease with Er content, except for the *c* parameter of the 2/17R phase that decreases as the Al content is increased.

The ranges of existence of the various phases are represented in Fig. 3 and can be summarized as follows. As the Al and R contents in the $R_2(Fe_{1-x}Al_x)_{17}$ series are increased the 2/17H phase transforms — usually via the 1/7H phase — into the 2/17R phase. While the former two phases dominate at or close to the 2/17 composition (9.5 and 10.5 at.% R), the latter phase dominates at higher R contents (11.5 at.%). This trend is consistent with the influence of geometrical factors on the structural stability of the rhombohedral phase (larger average atomic volume) and the hexagonal phase (smaller average atomic volume). As to the solubility of aluminum in the 2/17H phase it increases as the atomic size of R decreases (from $x=0$–3.42 in $Tb_2Fe_{17-x}Al_x$ to $x=0$–4.75 in $Er_2Fe_{17-x}Al_x$), while that in the rhombohedral phase decreases (from $x=7.70$–9.41 in $Tb_2Fe_{17-x}Al_x$ to $x=5.70$–7.03 in $Er_2Fe_{17-x}Al_x$). Thus aluminum substitution shifts the stability of the 2/17R phase towards smaller R con-

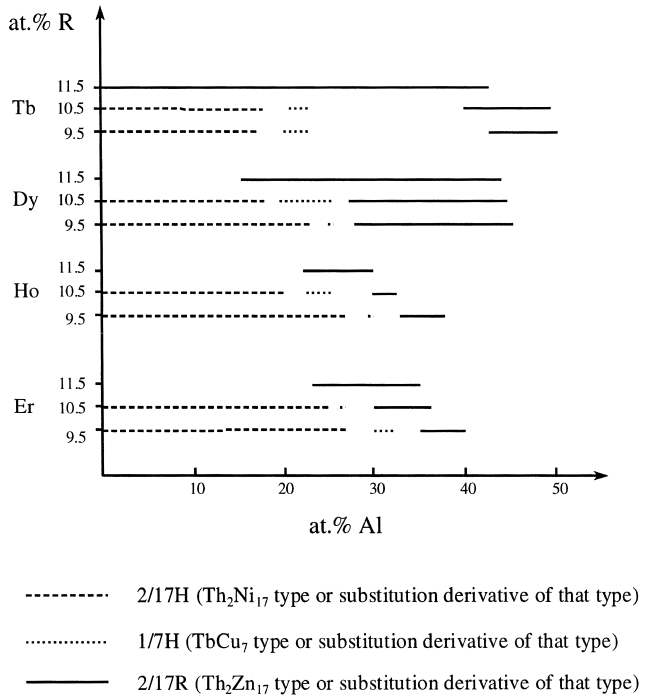

Fig. 3. Homogeneity ranges of the 2/17H, 1/7H and 2/17R phases in R–Fe–Al systems at various R contents (500°C).

centrations. In the binary (Dy, Ho, Er)–Fe systems no 2/17R phase appears, while in the ternary (Dy, Ho, Er)–Fe–Al systems the 2/17R phase appears only if a certain minimum amount of iron is substituted by aluminum. As expected, this minimum decreases as the atomic size of R is increased. In the La–Fe–Al system, for example, a binary 'La_2Fe_{17}' phase does not exist, and the critical Al concentration for the occurrence of the 2/17R phase is $La_2Fe_7Al_{10}$ [8]. A similar trend also occurs as a function of R content. For high R contents (11.5 at.% R) the 2/17R phase appears at lower Al contents, *x*, than for medium or low R contents (10.5 and 9.5 at.% R). Interestingly, the opposite trend occurs for the 2/17H phase for which the solubility of Al appears to decrease as the atomic size and content of R is increased. On the other hand, the solubility of Al in that phase increases as the annealing temperature is decreased. As to the 1/7H phase it covers the concentration range 20–30 at.% Al and is shifted to higher Al contents as the atomic size of R is decreased. In the Er system, for example, that phase appears at the composition $Er_2Fe_{11.3}Al_{5.7}$ (500°C), in contrast to the 2/17R structure that appears near the composition ($Er_2Fe_{12}Al_5$) in samples annealed at 1400 K [6]. A $TbCu_7$ type derivative structure and its transition to a 2/17R type derivative structure has recently been observed in the binary Sm–Fe system [9] at 750–800°C on samples prepared by mechanical alloying. The appearance of a $TbCu_7$ type derivative structure in the presently studied ternary systems at much lower annealing temperatures (500°C) is surprising because this structure is probably the most disordered among all structures considered. These results suggest that the annealing temperature plays an important role for the phase limits of the various $R_2(Fe_{1-x}Al_x)_{17}$ compounds.

Finally, the question arises as to what structural changes occur during the Fe and R substitutions. Clearly, compositional ratios R/(Fe,Al)$<$2/17 in Th_2Zn_{17} and Th_2Ni_{17} type structures favor R atoms to be substituted by Fe_2 dumbbells, whereas R/(Fe,Al)$>$2/17 favors the inverse (Fe_2 substituted by R). Both types of substitutions are known to occur at various degrees in 2/17 compounds and lead to the 2/17H derivative structure of $LuFe_{9.5}$ (R by Fe_2, and vice versa) and the 2/17R derivative structure of $PrFe_7$ (Fe_2 by R). As to the 1/7H structure it derives from the $CaCu_5$ type structure by partial substitution of R by Fe_2. Whether such substitutions also occur in the present series of compounds needs to be confirmed by detailed crystal structure analyses. The different concentration dependencies of the cell parameters, in particular *c*, suggest that the nature of these substitutions changes as a function of Al content, structure type and atomic size of R.

References

[1] Z. Cheng, B. Shen, Q. Yan, H. Guo, D. Chen, C. Gou, K. Sun, F.R. deBoer, K.H.J. Buschow, Phys. Rev. B 57 (1998) 14299.
[2] P. Villars, Pearson's Handbook. Desk Edition. Crystallographic Data for Intermetallic Phases, ASM International, Materials Park, OH, 1997, In 2 volumes.
[3] O.I. Bodak, E.I. Gladyshevskii, in: Ternary Systems with Rare Earth Metals, Vytscha Shcola, L'viv, 1985, p. 328, In Russian.
[4] S.R. Mishra, G.J. Long, O.A. Pringle, G.K. Marasinghe, D.P. Middleton, K.H.J. Buschow, F. Grandjean, J. Magn. Magn. Mater. 162 (1996) 167.
[5] D. Plusa, R. Pfranger, B. Wyslocki, J. Less-Common Metals 99 (1984) 87–97.
[6] T.H. Jacobs, K.H.J. Buschow, G.F. Zhou, X. Li, F.R. deBoer, J. Magn. Magn. Mater. 116 (1992) 220.
[7] A. Lefevre, L. Cataldo, M.Th. Cohen-Adad, B.F. Mentzen, J. Alloys Comp. 255 (1997) 161.
[8] W. Tang, J. Liang, G. Rao, Y. Guo, Y. Zhao, J. Alloys Comp. 218 (1995) 127.
[9] A. Teresiak, M. Kubis, N. Mattern, M. Wolf, K.-H. Müller, J. Alloys Comp. 274 (1998) 284.